

## **COBRA-IE: A NEW SUB-CHANNEL ANALYSIS CODE**

**D. L. Aumiller, G. W. Swartele, M. J. Meholic, L. J. Lloyd, F. X. Buschman**

Bettis Atomic Power Laboratory

PO Box 79

West Mifflin, PA 15122 USA

david.aumiller@unnpp.gov

### **ABSTRACT**

A variant from the COBRA-TF code series has been developed that incorporates many new features and enhances computational capability and accuracy. The new code, referred to as COBRA-IE, has been developed as a general purpose thermal-hydraulic analysis code, with an emphasis on analysis of Loss-of-Coolant Accidents (LOCA) when used in conjunction with an integrated code system using the PVMEXEC, RELAP5-3D, MELCOR, and CONTAIN programs. This paper provides an overview of the COBRA-IE code describing the advanced physical models and capabilities that have been developed and implemented in the code. Of particular note are the inclusion of the ability to treat non-condensable gases, the development of a three-field counter-current flow limitation (CCFL) model, implementation of mechanistic dispersed flow film boiling (DFFB) models, the development of RELAP5-3D compatible water properties, and the creation of several nonlinear solution algorithms. Finally, implementation of thermal-hydraulic, neutron kinetic and control system coupling in COBRA-IE is described.

### **KEYWORDS**

COBRA-IE, COBRA, Advanced Sub-Channel

### **1. INTRODUCTION**

The calculation of two-phase conditions for both steady-state and transient simulations is important to the ability to demonstrate the safe operation of nuclear power plants. The analytical codes that are used for these calculations vary from lumped parameter codes such as MELCOR [1], to two-phase system codes such as RELAP5-3D [2], TRACE [3] and ATHLET [4], to sub-channel analysis codes such as COBRA-TF [5] to multiphase CFD codes such as ANSYS CFX [6]. With each successive class in the previous list, the complexity of the physical models, size of the required analysis models and the computational run time are increased.

While active development of sub-channel analysis codes reached a nadir in the 1990's, more recently there has been a recognition that three-field analysis codes can fill a very important niche in bridging the gap between the two-field system analysis codes that have 100's of volumes and typical execution times range in the minutes to hours and two-phase CFD codes that require millions or billions of mesh points for problems that involve significant portions of the reactor core and required run times measured in days or weeks. As a result, there have been several new advanced three-field analysis codes such as CTF [7], F-COBRA-TF [8], MEFISTO [9] and CUPID [10], which eschew the sub-channel formulation for a more conventional unstructured mesh, that have been created recently.

During the past 15 years, the Bettis Atomic Power Laboratory has been developing their advanced sub-channel code, called COBRA-IE. The name has been selected to both indicate that it belongs to the COBRA-TF family and that it functions within PVMEXEC [11] Integrated Environment. This paper will

describe the various improvements made to the underlying physical models and to the mathematical methods in COBRA-IE. The various methods by which COBRA-IE has been coupled to RELAP5-3D and to an advanced Monte-Carlo simulation code are highlighted. Finally, the advanced verification and assessment methodologies that have been developed for use with COBRA-IE will also be discussed.

## **2. Improved Physical Models**

### **2.1. Improved Annular Flow Models**

Significant effort has been spent to increase the accuracy of the annular flow models within COBRA-IE [12]. The annular flow regime can be important to several different scenarios of importance to the thermal-hydraulic analysis of nuclear reactors. The calculation of dryout critical heat flux in Boiling Water Reactors is greatly influenced by the liquid film thickness that exists in the annular flow regime. Annular flow can also exist in a LOCA scenario in a nuclear reactor during both the blowdown and reflood phases. In low flooding rate scenarios, annular flow typically exists upstream of the dryout location. Excess liquid films can result in a more rapid quench front velocity and a shorter reflood transient time relative to the experimental data.

A physically based and self-consistent model set for co-current annular flow has been developed and assessed in COBRA-IE. This model has the following attributes: (1) applies an interfacial shear model (called the two-zone model) that explicitly accounts for the presence of interfacial waves, (2) idealizes the structure of the interface in a manner that is consistent with both the interfacial shear model and visual observations, (3) includes three mechanistically based entrainment rate models (roll wave stripping, Kelvin–Helmholtz lifting, and liquid bridge breakup) that calculate theoretical entrainment rate based on the governing phenomena as they are currently understood, and (4) provides a functional relationship between the actual and theoretical entrainment rates based on comparisons to experimental data. The self-consistent nature of the modeling package references the consistent use of parameters between the interfacial drag model, entrainment rate models, and flow regime map. For example, the disturbance wave height, velocity, and interfacial shear stress calculated by the two-zone model are used as input to the entrainment rate models. The inclusion of this package reduced the mean relative error in entrained fraction from 20.2% (underprediction) to 4.5% (overprediction), see Figure 1, and in axial pressure gradient, Figure 2, from 108.2% to 7.6% (both overprediction). For details of the data used in the comparison, see Reference [12].

### **2.2 Advanced Models for Dispersed Flow Film Boiling Heat Transfer**

Film boiling heat transfer is an important phenomenon for LOCA analyses. As a post-critical heat flux heat transfer regime in which the minimum film boiling temperature has been exceeded, film boiling is characterized by a continuous vapor contact with the heated surface and vapor generation at the liquid-vapor interface. Six different heat transfer paths must be considered in a DFFB model: two convective heat transfer paths, three radiative heat transfer paths and the heat transfer from the wall to the entrained droplets when they intermittently come into contact with the superheated wall. This last heat transfer path is referred to as direct or dry contact heat transfer. The most commonly implemented direct contact model within the nuclear industry is a version of the Forslund and Rohsenow [13] model. However, several of the models suggested by Forslund and Rohsenow are either inapplicable for nuclear reactor analysis or do not provide an accurate physical representation of the true situations. Lane *et al.* [14] provides a critical review of the Forslund and Rohsenow model and highlights a number of deficiencies in the model for application to reactor safety analysis. Some of the most important of the deficiencies include the use of a horizontal heat transfer coefficient yielding a gravitational dependence, being independent of the local flow conditions, and predicting unphysical results with respect to wall superheat.

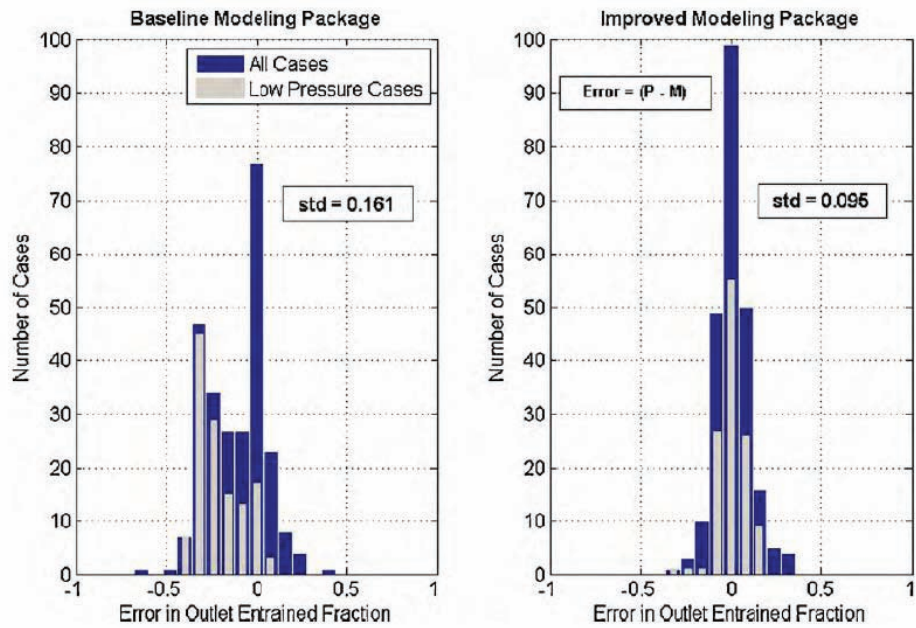


Figure 1 - Comparisons of Models for Entrainment

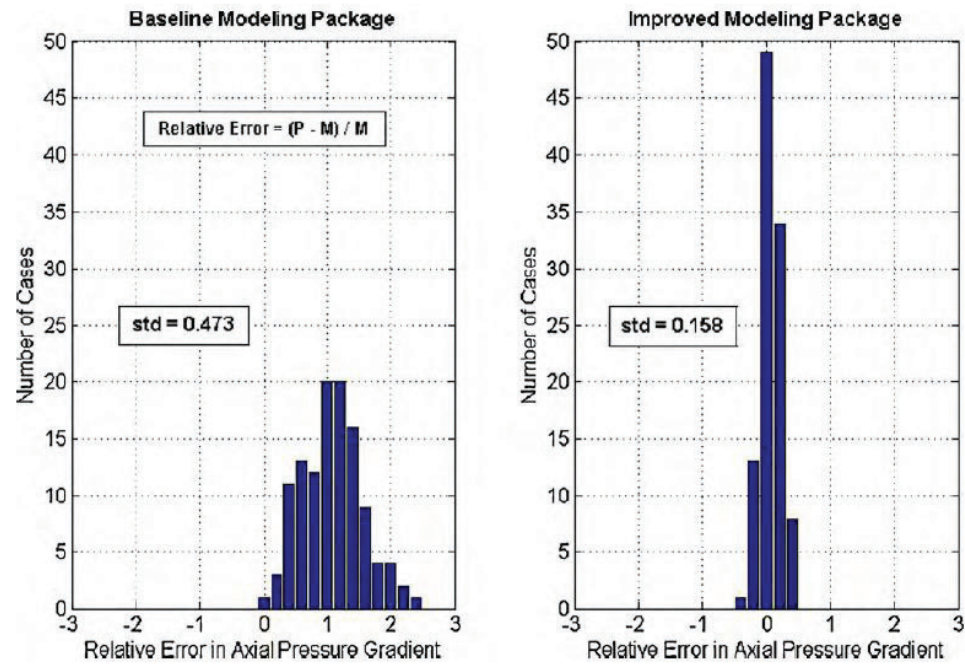


Figure 2 - Comparison of Models for Axial Pressure Gradient

To resolve these issues, a new DFFB model has been developed [15-17] for use in nuclear reactor safety analysis codes. The proposed model improves upon previous DFFB models by correcting prior modeling deficiencies and implements a number of novel developments. Some of the advances in the proposed model over previous models were the implementation of a physically based, subscale Lagrangian trajectory calculation to determine if a droplet can intermittently contact the wall, the inclusion of a droplet size distribution across all of the calculations and the development of a novel, two-phase

convective enhancement factor. The trajectory calculation tracks the drops through the vapor boundary layer in two-dimensions and includes the following forces: drag, body force, lift, and a differential evaporation (or thrust) force. This physically links the direct contact heat transfer to the local conditions (i.e., vapor mass flux, wall superheat, and vapor superheat).

The DFFB heat transfer package was assessed against various sets of experimental data. The assessment was specifically focused on steam-water experimental data in vertical tubes. The choice to only examine steam-water data was made given that the model was specifically developed for use in nuclear reactor safety analysis codes. Additionally, the use of only vertical tube experiments rather than including rod bundle experiments was made to provide a baseline without examining the numerous effects of spacer grids on DFFB heat transfer. These include their effect on the droplet size spectrum and the ability of spacer grids to quench in advance of the quench front and de-superheat the surrounding vapor. A total of 118 steady-state experimental runs were utilized in the assessment. The Royal Institute of Technology (RIT) [18], Bennett [19], and CISE [20] experiments were all uniformly heated while the Harwell [21] experiments utilized a cosine power shape.

The resulting errors from the assessment were examined for any biases based upon the local conditions as well as the fraction of the heat transfer attributed to each DFFB heat transfer component. No large biases were observed with the proposed DFFB model. Figure 3 compares the resulting wall superheats for both DFFB models to the experimental wall superheats across all of the experimental data. Overall, the proposed DFFB model reduced the mean error from 27.36 K to -14.27 K while almost cutting the standard deviation in half from 82.15 K to 44.75 K. Additionally, the RMS error was reduced from 86.56 K to 46.96 K across all of the experimental data points. Additionally, the trend of over predicting wall superheats as the measured wall superheat increases has been removed with the proposed model.

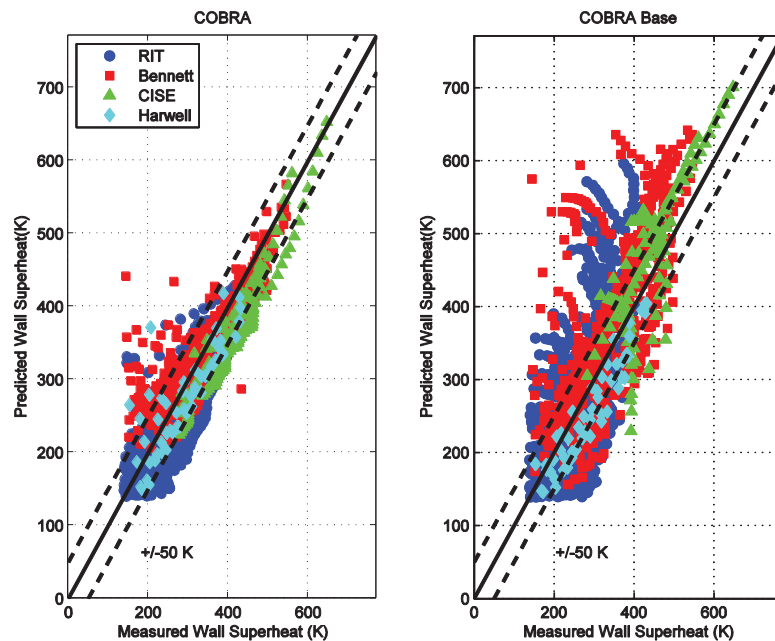


Figure 3 – Comparison of New DFFB and Previous COBRA-TF DFFB Model to Data

### 2.3 Three-Field Counter Current Flow Modeling

A three-field Counter-Current Flow Limitation (CCFL) model based on the classic flooding curve methodology has been developed and successfully demonstrated in COBRA-IE [22]. The various physical mechanisms (wave reversal, liquid bridging, and wave interfacial instability) that govern the

flooding and flow reversal phenomena are extremely complex and geometry dependent. As a result, universally applicable numerical models for these phenomena are not currently available. The chosen approach provides flexibility and leverages the available experimental data to improve the predictive capability of the code. The model is an extension of the standard two-field (liquid-vapor) CCFL model to three-fields (liquid films, vapor and liquid droplets). This extension includes providing the appropriate set of momentum equations, definitions of required superficial velocities, and new entrainment correlations based on CCFL conditions. Necessary criteria to enter and exit the model in a numerically stable manner were also developed.

The Wallis [23] or Kutateladze[24] forms of the CCFL correlation can be written in a generic form as:

$$H_v^{1/2} + mH_l^{1/2} = C \quad (1)$$

where both  $m$  and  $C$  are derived from flooding data. Since the solution variable in COBRA-IE is the phasic mass flow rate ( $W_k$ ), it is desired to write the dimensionless parameters ( $H_k$ ) in terms of this variable, rather than the superficial velocity, such that:

$$H_k = Y_k W_k \text{ for } k=l \text{ or } v \quad (2)$$

where:

$$Y_k = \frac{1}{A_x} \sqrt{\frac{1}{g \Omega \rho_k \Delta \rho}} \quad (3)$$

Similar to the RELAP5-3D [13] implementation, the weighting parameter ( $\Omega$ ) in this expression is given as:

$$\Omega = L_w^{1-\beta} \left( \sqrt{\frac{\sigma}{g \Delta \rho}} \right)^\beta \quad (4)$$

where the Wallis length scale ( $L_w$ ) is a user input parameter. In this formulation if  $\beta=0$  and the Wallis length scale is equal to the hydraulic diameter, the Wallis form of the CCFL equation is obtained and if  $\beta=1$  then the Kutateladze form of the CCFL equation is obtained.

The unique aspect of developing a dedicated CCFL model for three-field analysis tools is the treatment of the entrained liquid field. Visual observations indicate the presence of entrainment at the CCFL location such that some of the liquid that does not penetrate downwards in the form of a falling film is swept upwards away from this location in the form of liquid droplets. Explicitly accounting for the existence of this entrainment mechanism also improves the numerical stability of the model as it provides a means for removing liquid from the CCFL location instead of allowing it to pool. Without an entrainment mechanism, water pools above the CCFL location until flow regime transitions provide enough interfacial drag to blow the liquid slug upward. The resulting “slugging” behavior prevents a stable solution.

Two different entrainment mechanisms are postulated for CCFL situations. If the postulated CCFL location corresponds to a flow area expansion, such as an upper tie plate, an inverted liquid pool will likely develop and a pool entrainment type mechanism will exist. A pool entrainment mechanism consists of vapor flowing through a stagnant liquid pool and entraining droplets from the pool surface. The flow within the bubbling pool can be described as churn-turbulent where droplets are created by a momentum exchange mechanism between the faster moving vapor and the stagnant liquid [25]. If no area change exists at the CCFL location, an excess film flow entrainment model is applied. This model

compares the continuous liquid volume fraction to a critical value and entrains the excess liquid. Both of these entrainment mechanisms have been added to COBRA-IE.

To show that this new model option can significantly improve the accuracy of counter-current flow calculations provided a flooding curve is available, an analysis of the Dukler & Smith [26] low-pressure air-water experiments is presented. In this test, Dukler & Smith measured pertinent flow rates, pressure gradients, and liquid film thicknesses within the flooding region. Figure 4 compares the experimental results published by Dukler & Smith for a liquid injection rate of 113 kg/hr to the predictions obtained with and without a CCFL boundary condition. Since the flow rates were measured at the inlet and outlet of the test section, the experimental data and the corresponding predictions reflect the integral effect of both the counter-current and co-current annular flow regimes. Figure 4 compares the predicted liquid downflow rates to the measured values. Significant improvement in the agreement with the experimental data was obtained following the implementation of an appropriately defined CCFL boundary condition. The difference between the experimental data and the predictions is a reflection of the accuracy of the fit of the flooding curve to the experimental data.

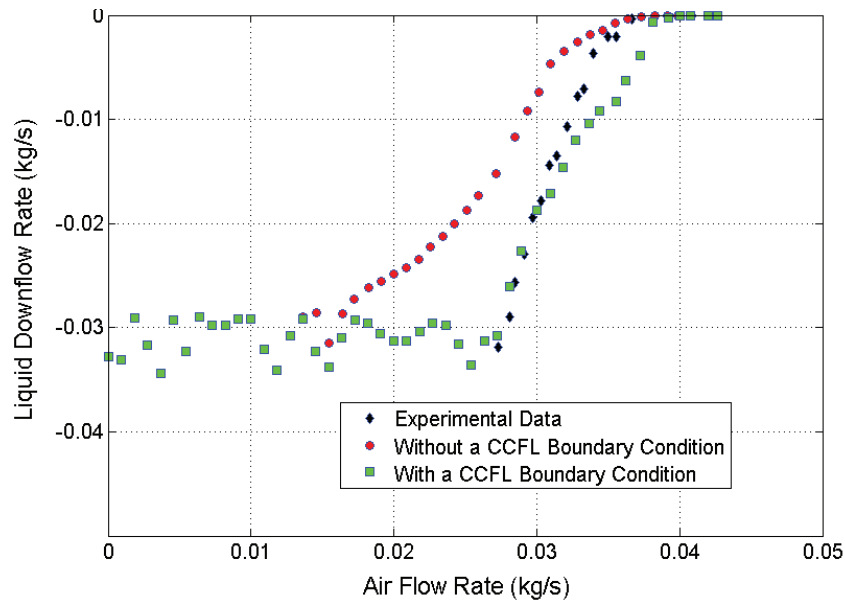


Figure 4 – CCFL results for Dukler-Smith Experiment

## 2.4 Additional Improvements

For the purpose of brevity, all of the modifications made during the development of COBRA-IE to improve the accuracy of the physical models can not be discussed in the same detail as the three models above. This section will provide a shorter description of some of the other changes that have been made.

The most pervasive change to the code has been to replace the original set of water properties with values that are more consistent with those from RELAP5-3D [2]. As described later, COBRA-IE has been coupled to RELAP5-3D. The use of consistent water properties provides stability to the coupled calculation since the phasic densities and temperatures, as well as the saturation temperature will be similar at the coupling location. This has been accomplished via the use of bi-cubic splines in COBRA-IE where the knot points are taken from the RELAP5-3D code. The RELAP5-3D routines could not be used, directly, since they are based on internal energy vice enthalpy as required by COBRA-IE. An iterative process is used to find the appropriate internal energy values required for the knot points.

Non-condensable gases from accumulators and containment can significantly impact the evolution of a LOCA. The version of COBRA-TF that was used as the starting point for COBRA-IE claimed to have the ability to track non-condensable gases. This feature had many errors in the implementation rendering the code very difficult to use even for problems that did not include non-condensables. During the COBRA-IE development, the temporal derivatives of the mass and energy equations and the interfacial heat transfer package were rewritten to correct the previous errors. The result is a code that is much more robust than its predecessor, and now contains an evaporation heat transfer mode for conditions where  $T_{dp} < T_l < T_{sat}$ . Furthermore, the previous code did not include a model for the suppression of condensation due to the presence of non-condensables. This has also been accounted for in COBRA-IE.

Additionally, a new model has been developed to solve a simplified set of equations appropriate for application to small, tortuous flow paths. This leakage path model assumes 1) mechanical equilibrium between the liquid and vapor, 2) no entrained droplets are permitted to flow through such areas and 3) no momentum can be advected to, through or from the leakage path. This model has provided significant accuracy and numerical stability to the solutions when such regions are present.

The hydraulic diameter of flow passages has been seen to influence interfacial dynamics differently when the hydraulic diameter is of the same order as bubble sizes [27] and when the diameter is as at least an order of magnitude larger than the bubble sizes [28]. To permit this behavior, COBRA-IE has added model sets for all three scenarios: small regions, intermediate regions and large open regions. These various models sets allow for additional accuracy when the code is applied to each scenario.

Additional improvements to the hydraulic solution methods include the ability to include the effects of roughness on wall drag through the use of the Zigrang-Sylvester correlation [31], the ability to input independent forward and reverse flow loss coefficients and the ability to read boundary condition from ascii files to permit the use of experimental data files to drive boundary conditions.

The heat transfer models have been improved by adding new correlations for the minimum film boiling temperature and for critical heat flux. The boiling curve methodology in COBRA-IE has been modified to include use of the Steiner-Taborek [29] model for prediction of the onset of nucleate boiling. Additionally, all of the terms in the boiling curve are now calculated on a heat structure surface instead of having some parameters, such as CHF, depend only on fluid conditions and not local heat structure conditions. The use of the Gnielinski correlation [30] also permits the wall roughness to impact heat transfer calculations.

### **3. Improved Mathematical Models and Programming Techniques**

#### **3.1 Nonlinear and Selective Nonlinear Solution Algorithms**

As described in Reference [32], COBRA-IE has been modified to solve the coupled nonlinear set of conservation equations as a nonlinear system vice using the traditional linear system approximations made in other versions of COBRA-TF. Not resolving the nonlinearities present in a simulation was shown to result in situations where timestep-size insensitivity was not the result of temporal convergence, but was an artifact of the degraded order of temporal accuracy caused by linearizing the discrete nonlinear equations. This insensitivity of the solution to timestep size refinement can be erroneously taken as an indicator of a temporally converged solution.

As part of the nonlinear solver, an operator-based scaling that provides a physically meaningful convergence measure is used. This operator-based approach allows for a scaling of the residual that eliminates inherent bias due to the order of magnitude of the terms in the equations; as such, this localized

scale factor normalizes its residual equation to between zero and one. The use of this scale factor is integral to the effective use of the nonlinear solver.

Until the nonlinear truncation error is eliminated by using an iterative solver, temporal convergence of the solution cannot be assured. However, in situations where nonlinearities are low, the solution produced by a single Newton iterate can be as accurate as that produced by the iterative solver with more stringent convergence tolerances. In many problems of interest, the dominant nonlinearities are spatially isolated to small portions of the domain. By selecting those areas of the domain where the nonlinearities are expected to be high and subjecting only them to multiple nonlinear iterations, the accuracy of the nonlinear solver is obtained without its associated computational cost. To allow for the resolution of these nonlinearities, a spatially selective, nonlinear refinement (SNR) algorithm was developed and implemented in COBRA-IE.

The SNR algorithm in COBRA-IE allows for an arbitrary subdomain of the problem to be specified as nonlinear. The linear and the nonlinear domains are coupled so as to achieve a consistent solution through the course of a given timestep. The nonlinear domain is subjected to multiple Newton iterates until convergence in that domain has been achieved. This SNR algorithm allows for the accuracy of the nonlinear solver to be achieved while reducing the total computational costs

As an evaluation of the SNR algorithm, a simple LWR model was developed. This simulation modeled the refill portion of LOCA scenario. The impact of timestep size on the integrated condensation from the safety injection nozzle in the upper head for the different methods is shown in Figure 5. As expected, the nonlinear solver demonstrated a more temporally converged solution than the linear solver. The linear solution also appears to converge to a different solution than that obtained by the nonlinear solver. The SNR algorithm provided results similar to the nonlinear case with one-third the computational effort. This problem demonstrates that the SNR algorithm can be useful in obtaining nonlinearly and temporally converged safety simulations with less computational cost than the traditional nonlinear solver.

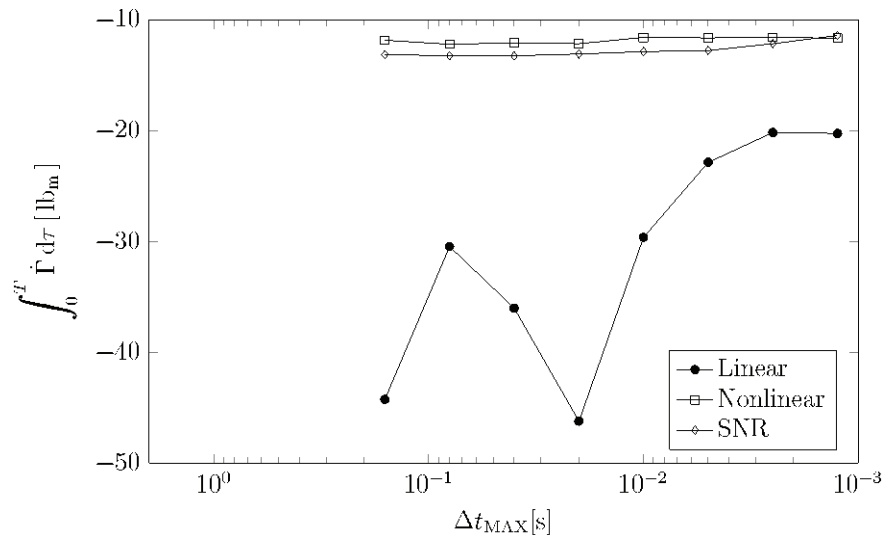


Figure 5 – Temporal Convergence of Linear, Nonlinear and SNR Solver for Calculated Condensation

### 3.2 Additional Mathematical Changes and Programming Techniques

COBRA-TF contained a domain decomposition solution algorithm for the solution of the linear system for the new time pressure. For this solver, the user would specify the bandwidth of the matrix solve, the

locations of the various simultaneous solution groups, the maximum number of iterates and the convergence criterion. It was seen that the user selections for these parameters could have a significant impact on the solutions generated. To provide a solution algorithm that was insensitive to user selections, the solutions algorithms were replaced with two different direct solve techniques. The first option is a direct matrix inversion. This solver is best suited to problems of small size. For larger problems, the SuperLU solver [33] has been implemented. For problems of modest size, 3000 volumes, the use of this solver in place of the direct solver yielded an overall code speedup of a factor of 6 while still providing the same solution as using direct matrix inversion.

In order to provide a source of numerical stability, thermal hydraulic codes such as COBRA-IE under-relax terms such as the heat transfer coefficients and drag. The purpose of the under-relaxation is to prevent the terms from changing by orders of magnitude over the course of a single timestep. These drastic changes can be caused by such events as the change in the flow regime or heat transfer regime in a given cell. One characteristic of such methods is that the time smoothing effect should not introduce an effect that changes with differing timestep sizes. The previous version of COBRA-TF included several techniques for time-smoothing parameters. All of the previous methodologies resulted in processes that were directly linked to the timestep size used. The previous methods have been replaced with the following technique which is timestep size independent

$$\phi^{n+1} = \left( e^{-\frac{\Delta t}{\tau}} \right) \phi^n + \left( 1 - e^{-\frac{\Delta t}{\tau}} \right) \tilde{\phi}^{n+1} \quad (5)$$

where  $\phi^{n+1}$  is the effective new time parameter,  $\tilde{\phi}^{n+1}$  is the parameter as calculated using latest conditions,  $\phi^n$  is the previous value of the parameter (which includes time smoothing in previous timesteps),  $\Delta t$  is the timestep size, and  $\tau$  is the time constant for the associated phenomenon.

Furthermore, the version of COBRA-TF that was used as the starting point for COBRA-IE was statically allocated which meant that maximum problem size was fixed during code compilation. This has been revised in COBRA-IE such that a dynamic process is used to determine the problem size and allocate the required memory structure. Additionally, as received, there was no ability to perform a restart of a COBRA-TF simulation. This capability has been added to COBRA-IE to permit long running transients such as LOCA's to be restarted at various points in the transient to modify conditions in the simulation or perform sensitivity studies.

#### 4. Verification and Validation Processes

Bettis has developed an extensive verification and validation process for use with COBRA-IE. This process has been documented in Reference [34]. It is a process that provides quantitative and qualitative metrics that demonstrate that code features are working as intended for each code release. Included in the assessments are assurances that the restart process and the timestep backup processes do not artificially impact the solution of COBRA-IE. Many errors in the timestep backup process were identified and resolved during this phase of code development. The methods have been adapted to show that the nonlinear solver with a single iteration and the linear solver return exactly identical solutions for every problem in the verification suite. To check that all combinations of solvers and backup types are tested, a total of six executions are performed for each verification problem. The linear and nonlinear solvers are each used to run the base case, a case backing up every hydraulic solution, and a case backing up every complete timestep. The results from all six cases must match to demonstrate proper code functionality.

## 5. Integration in Coupled Code System

The PVMEXEC executive [11] has been jointly developed at the Idaho National Laboratory and the Bettis Atomic Power Laboratory to overcome the shortcomings associated with previous, code-to-code coupling efforts. This tool has been developed to provide stable and generic coupling interfaces to permit integrated analyses that require thermal-hydraulic, reactor kinetics or neutronics, or control system information to be passed between different analysis codes.

COBRA-IE has been successfully integrated into the PVMEXEC system to provide new analytical capabilities for COBRA-IE analyses. This section will provide a brief description of the various coupling capabilities that have been added and will provide the results from two sample calculations.

### 5.1 Semi-Implicit Coupling

Using the nomenclature of Weaver [35], the semi-implicit coupling methodology uses a master-slave relationship where the mass and energy equations for the volume attached to the coupling location in the master computational domain is modified by retaining the mass, energy, volume and non-condensable gas flow rates as unknowns. These terms are retained as additional right hand sides when the final pressure matrix is developed. By retaining these terms, the changes in the pressures in all of the volumes in the computational domain can be computed in terms of the flow rates in the coupling junctions as:

$$\begin{aligned} \delta P_k^{n+1} = & a_k + \sum_{j=1}^{N_c} b_{k,j} \dot{m}_{g,j}^{n+1} + \sum_{j=1}^{N_c} c_{k,j} \dot{u}_{g,j}^{n+1} + \sum_{j=1}^{N_c} d_{k,j} \dot{u}_{f,j}^{n+1} \\ & + \sum_{j=1}^{N_c} e_{k,j} \dot{m}_{g,j}^{n+1} + \sum_{j=1}^{N_c} f_{k,j} \dot{m}_{f,j}^{n+1} + \sum_{j=1}^{N_c} g_{k,j} \dot{w}_{g,j}^{n+1} + \sum_{j=1}^{N_c} h_{k,j} \dot{w}_{f,j}^{n+1} \end{aligned} \quad (6)$$

where  $\dot{m}_g$ ,  $\dot{u}_g$ ,  $\dot{u}_f$ ,  $\dot{m}_g$ ,  $\dot{m}_f$ ,  $\dot{w}_g$  and  $\dot{w}_f$  represent the flow rate of non-condensable gas, and the phasic flow rates of energy, mass and volume at the coupling locations, and  $N_c$  is the number of coupling junctions. The coefficients  $a$  through  $h$  for the volumes attached to the coupling junctions are then transmitted to the slave code that uses coefficients  $a$  through  $h$  to calculate the interdependence of pressure and flow rates consistent with the algorithm used in the master code. This consistency is the key to the semi-implicit coupling methodology. When the mass, energy, volumetric and non-condensable flow rates in the coupling junctions have been received from the slave process, Equation (6) can be evaluated for the change in the pressure in each volume in the master code. Once the changes in the pressures in the volumes have been computed, the time advancement may be completed in the normal manner.

COBRA-IE has been added to the PVMEXEC code system as a slave process [36]. Through the use of the RELAP5-3D analysis code [2] to model all reactor systems except the reactor vessel, COBRA-IE is now capable of being used to model transients where the entire plant response is important. An example of such a scenario would be the analysis of a LOCA. Such an analysis was performed of the Loss of Fluid Test (LOFT) L2-5 experiment [37, 38]. The analysis which is presented in more detail in Reference [39] is summarized here. In this simulation, a COBRA-IE model was constructed of the LOFT facility reactor vessel. This was coupled to the RELAP5-3D model at each of the four nozzles.

The most important metric used to evaluate the accuracy for LOCA simulations is the predicted fuel rod clad temperature. A comparison of the predicted fuel clad temperature for the center region of the reactor is shown in Figure 6. This comparison shows two different temperature measurements from pins D7 and

I4 at an elevation of 0.69 meters. This elevation was chosen because it was both among the hottest locations measured and it included the longest quench time. The results shown in Figure 6 indicate that the coupled code system that has been developed around PVMEXEC is capable of predicting clad temperatures and the quench time for the LOFT test facilities in an accurate manner.

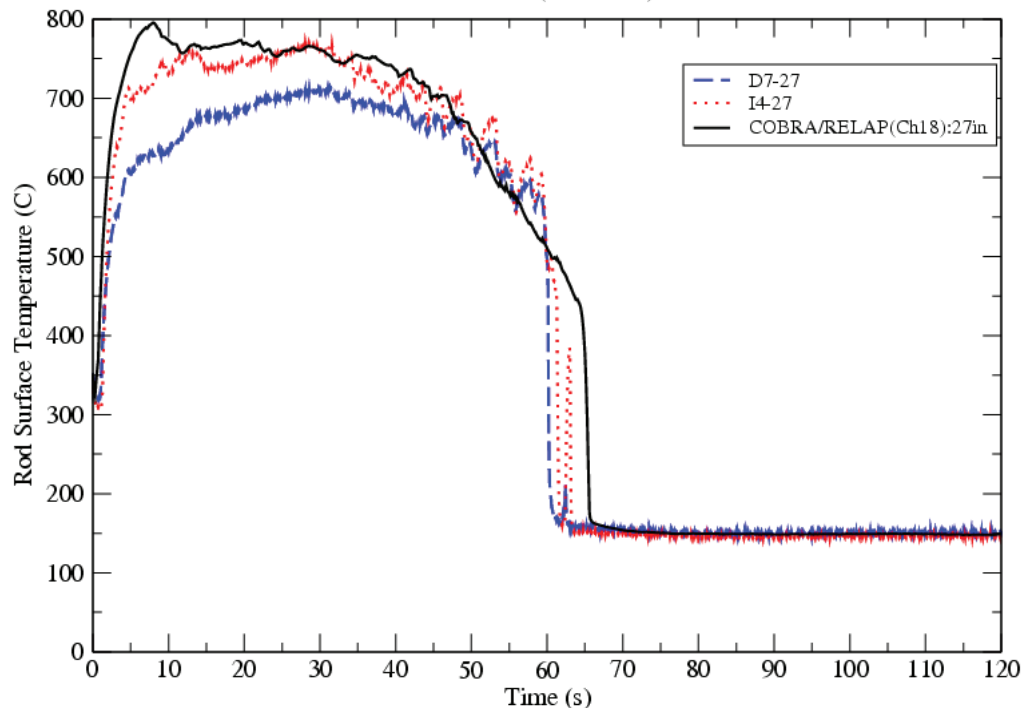


Figure 6 – COBRA-IE Predictions of Clad Temperature from LOFT L2-5 Experiment

## 5.2 Kinetics Coupling

The ability to calculate both spatially and time varying power profiles is of primary importance to many analyses of interest to thermal-hydraulic analysis codes such as COBRA-IE. For application to a LOCA, it is required to be able to calculate the reduction in power as the core voids and the decay heat as a function of time. Previous versions of COBRA-TF required the user to input tables with tables of power versus time. This is insufficient since the void fraction in the core and the core power depend on each other. Additionally, COBRA-TF only permitted the user to change the power level, and not the power shape, to change during a simulation. To permit the ability to provide both time and space varying power shapes, COBRA-IE uses the kinetics coupling option in PVMEXEC. In this technique, the fluid density, temperature and boron concentration are sent from COBRA-IE to a code that will perform neutronic calculations. This technique has been used to couple COBRA-IE to RELAP5-3D. This combination has been used to exploit the point kinetics and decay heat models in RELAP5-3D for application to LOCA simulations. By using the coupling approach, vice developing a standalone capability for COBRA-IE, resulted in a significant reduction in development and verification resources.

More recently, COBRA-IE has been coupled with the advanced Monte Carlo code, MC21 [40]. This coupled code system is capable of providing detailed power and thermal-hydraulic calculations. An example to demonstrate MC21-COBRA coupling has been performed for a PWR assembly (utilizing eighth-assembly symmetry). The model contained a total of 864 fuel temperature regions, 1512 sub-channel regions and 1008 power producing regions. The planar slice shown in Figure 7 shows the

distribution of coolant density and integrated pin power in the assembly. The observed trends agree with physical intuition, specifically that the most power is produced in rods surrounding the relatively cold guide tubes. The sink densities near the guide tubes support this observation.

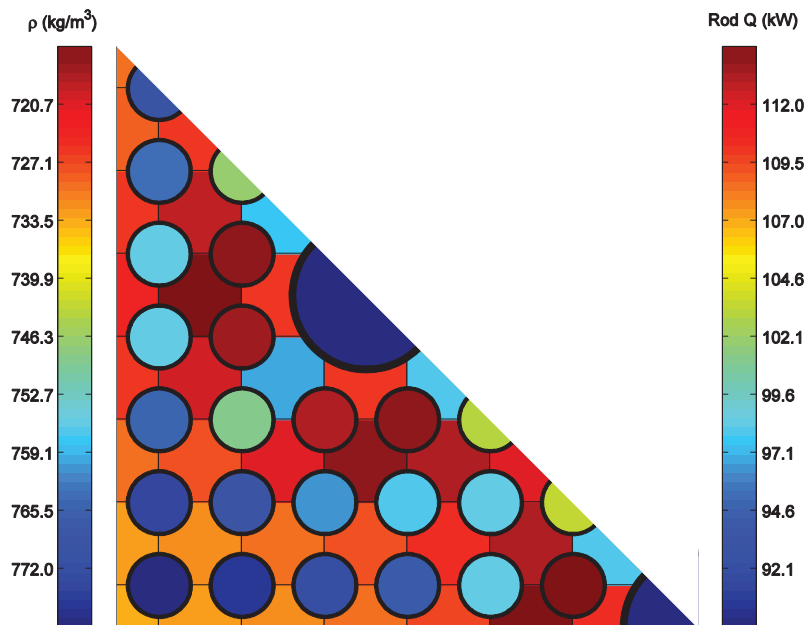


Figure 7 – Coupled COBRA-IE MC21 Analysis of a 1/8<sup>th</sup> Assembly

### 5.3 Control System Coupling

COBRA-IE contains no intrinsic control system capability. To provide this required feature, the program has been modified to work with the control system coupling capability of PVMEXEC. COBRA-IE can both send generic solution data to other codes and receive data from those codes to drive boundary conditions within the simulation. For instance, COBRA-IE can send pressure signals from the simulation to feed simulated plant control system logic. Additionally, the control system coupling can be used to simulate a drain system that maintains a constant level modifying a transient flow area model, which has been added to COBRA-IE. In this example, COBRA-IE would send the required void fractions to RELAP5-3D, where the new area would be calculated and sent back to COBRA-IE. Control system coupling provides significant additional flexibility and capability to analyses that use COBRA-IE.

### 6 Conclusions

The COBRA-IE subchannel analysis code has been developed to resolve many of the previous errors and difficulties associated with such tools. Many improvements have been made; several of the more significant modifications have been described: an advanced self consistent annular flow package, an Eulerian-Lagrangian method for DFFB calculations and a three-field CCFL model. Additionally, COBRA-IE is now capable of solving problems where non-condensable gases are present.

Significant modifications have also been made to the mathematical modelling used in COBRA-IE. The implementation of both a full nonlinear solver and the SNR method in COBRA-IE represents a significant advancement in the field. An example was shown where the typical solver techniques “converges” to the incorrect value, while the SNR method converges to the same answer as the fully nonlinear solver using one-third of the solution time.

The integration of COBRA-IE within the PVMEXEC code system was demonstrated. A few sample calculations were provided to highlight the capability that is created when COBRA-IE is coupled to a plant analysis code to permit its use in LOCA simulations and its ability to be used to perform high fidelity coupled simulations of power distribution within a PWR assembly.

## REFERENCES

1. R.O. Gauntt, et al., "MELCOR Computer Code Manuals – User's Manual", NUREG/CR-6119 Rev 3., SAND2005-5713, Sandia National Laboratories, 2005
2. The RELAP5-3D Code Development Team, "RELAP5-3D Code Manual Volume I: Code Structure, System Models and Solution Methods," INL-EXT-98-00834-V1, June, 2012.
3. TRACE V5.0 Theory Manual, "Field Equations. Solution Methods, and Physical Models", USNRC, Washington DC.
4. V. Teschendorff, H. Austregesilo and G. Lerchl, "Methodology, Status and Plans for Development of and Assessment of ATHLET", Proceedings of OECD/CSNI Workshop on Transient Thermal-Hydraulic and Neutronic Codes Requirements", Annapolis Md (1996)
5. M. J. Thurgood, J. M. Kelly, et al., "COBRA/TRAC – A Thermal-Hydraulics Code for Transient Analysis of Nuclear Reactor Vessels and Primary Coolant Systems – Equations and Constitutive Models," *NUREG/CR-3046*, Vol. 1, United States Nuclear Regulatory Commission (1983).
6. ANSYS Inc, "ANSYS CFX Solver Theory Guide", (2009).
7. M. Avramova and Diana Cuervo, "Assessment of CTF Boiling Transition and Critical Heat Flux Modeling Capabilities Using the OECD/NRC BFBT and PSBT Benchmark Databases", *Sci and Tech of Nucl. Inst.*, **2013**, Article ID 508485, (2013)
8. M. Gluck. "Subchannel Analysis with F-COBRA-TF – Code Validation and Approaches to CHF Prediction". *Nuclear Engineering and Design*, **237**, pp 655-667, (2007).
9. C. Adamson and J-M Le Corre "MEFISTO – A Mechanistic Tool for the Prediction of Critical Power in BWR Fuel Assemblies", Proceedings of ICONE-16, Paper ICONE16-48703, Orlando FL (2008).
10. J.J. Jeong, et al, "A Semi-Implicit Numerical Scheme for Transient Two-Phase Flows", *Nuclear Engineering and Design*, **238**, pp 3403-3412, (2010).
11. W.L Weaver, E.T Tomlinson, and D.L Aumiller, D. L., "An Executive Program For Use with RELAP5-3D", Proceedings of ICONE-10 or American Nuclear Society, Arlington VA (2002).
12. J.W. Lane, D.L. Aumiller, L.E. Hochreiter, and F.B. Cheung "A Self-Consistent Three-Field Constitutive Model Set for Predicting Co-Current Annular Flow," *Nuclear Engineering and Design*, **240**, pp 3294- 3308 (2010).
13. R.P. Forslund and W.M. Rohsenow, "Dispersed Flow Film Boiling," *Journal of Heat Transfer*, **90**, pp. 399-407, (1968).
14. Lane. J. W., Hochreiter, L. E., and Aumiller, D. L., "Critical Review of the Dispersed Flow Film Boiling Heat Transfer Model Suggested by Forslund and Rohsenow," *Proceedings of the 12th International Topical Meeting on Nuclear Reactor Thermal-Hydraulics (NURETH12)*, Pittsburgh, Pennsylvania, (2007).
15. M.J. Meholic, "The Development of a Non-Equilibrium Dispersed Flow Film Boling Heat Transfer Modelling Package," PhD Dissertation, The Pennsylvania State University, Department of Mechanical and Nuclear Engineering, 2011.
16. M.J. Meholic, D. L. Aumiller1 and F. X. Cheung, "A Comprehensive, Mechanistic Heat Transfer Modeling Package For Dispersed Flow Film Boiling – Part 1 - Development" Proceedings of NURETH-15, Paper NURETH15-114 . Pisa, Italy,(2013)
17. M.J. Meholic1, D. L. Aumiller1 and F. X. Cheung, "A Comprehensive, Mechanistic Heat Transfer Modeling Package For Dispersed Flow Film Boiling – Part 2 – Implementation And Assessment" Proceedings of NURETH-15, Paper NURETH15-115, Pisa, Italy,(2013)
18. Becker, K. M., et al., "An Experimental Investigation of Post Dryout Heat Transfer," Royal Institute of Technology, Report KTH-NEL-33, Stockholm, Sweden, (1983).

19. Bennett, A. W., Hewitt, G. F., Kearsley, H. A., and Keeys, R. K. F., "Heat Transfer to Steam-Water Mixtures Flowing in Uniformly Heated Tubes in Which the Critical Heat Flux Has Been Exceeded," United Kingdom Atomic Energy Authority, AERE-R5373, (1967).
20. Barzoni, G. and Martini, R., "Post-Dryout Heat Transfer: An Experimental Study in Vertical Tube and Simple Theoretical Method for Predicting Thermal Non-Equilibrium," 7th International Heat Transfer Conference, Munich, Germany, Heat Transfer, Vol. 5, pp. 411-416, (1982).
21. Keeys, R. K. F., Ralph, J. C., and Roberts, D. N., "Post Burnout Heat Transfer in High Pressure Steam Water Mixtures in a Tube with Cosine Heat Flux Distribution," United Kingdom Atomic Energy Authority, AERE-R6411, (1971).
22. J.W. Lane, D.L. Aumiller, L.E. Hochreiter, and F.B. Cheung, "Three-Field Counter-Current Flow Limitation Model," *Nuclear Technology*, **177**, pp. 176-187 (2012).
23. G. Wallis: *One-Dimensional Two-Phase Flow*, McGraw-Hill, New York (1969).
24. Kutateladze: "Elements of the Hydrodynamics of Gas-Liquid Systems", *Fluid Mechanics-Soviet Research*, **1**, pp. 29-50 (1972).
25. I. Kataoka and M. Ishii, "Mechanistic Modeling and Correlations for Pool-Entrainment Phenomenon," *NUREG/CR-3304, ANL-83-37*, Argonne National Laboratory, Argonne, IL (1983)
26. A. Dukler and L. Smith, "Two-Phase Interactions in Countercurrent Flow: Studies of the Flooding Mechanism," *NUREG/CR-0617* (1979).
27. M.J. Holowach, "The Development of a Reflood Heat Transfer Computational Package for Small Hydraulic Diameter Geometries", Master Thesis, The Pennsylvania State University, (2000).
28. J.M. Putney, "Development of a New Bubbly-Slug Interfacial Friction Model for RELAP5", *Nuclear Engineering and Design*, **131**, pp 223- 240 (1991).
29. J. Collier and J. Thome, *Convective Boiling and Condensation*, McGraw-Hill, New York (1996).
30. V. Gnielinski, "New Equations for Heat and Mass Transfer in Turbulent Pipe and Channel Flow," *Int. Chem. Eng.*, **16**, pp. 359-368 (1976)
31. D.J. Zigrang and N.D. Sylvester, "Explicit Approximations to the Friction Factor", *AIChE J*, **28**, 514-515, (1982).
32. L.J. Lloyd, "Development of a Spatially-Selective, Nonlinear Refinement Algorithm for Thermal-Hydraulic Safety Analysis", PhD Thesis, University of Wisconsin, (2014).
33. J.W. Demmel, et al, "A Supernodal Approach to Sparse Partial Pivoting", *SIAM J. Matrix Analysis and Applications*, **20**, pp 720-755, (1999).
34. D.L. Aumiller, et al, "Development of Verification Testing Capabilities for Safety Codes", *Proceedings of NURETH-15*, Paper NURETH15-145, Pisa, Italy (2013).
35. W.L Weaver, E.T. Tomlinson, E. T. and D. L Aumiller, "A Generic Semi-Implicit Coupling Methodology For Use In RELAP5 3D©," *Nuclear Engineering and Design*, **211**, pp. 13-26 (2001).
36. D.L. Aumiller, E.T. Tomlinson and R.C. Bauer, "Incorporation of COBRA-TF in an Integrated Code System with RELAP5-3D Using Semi-Implicit Coupling," Proceeding of 2002 RELAP5 International User Seminar, Park City Utah (2002).
37. D.L. Reeder, "LOFT System and Test Description (5.5-FT Nuclear Core 1 LOCES)", NUREG/CR-0247 TREE-1208, EG&G Idaho Inc., (1978).
38. P.D. Bayless, "Experiment Data Report For LOFT Large Break Loss-of-Coolant Experiment L2-5", NUREG/CR-2826, EG&G Idaho Inc., (1982)
39. J.G. Williams "Large Break LOCA Analysis Using a Coupled COBRA-TF/RELAP5-3D Best-estimate Computer Code Package: Simulation Of The Loft Facility Experiment L2-5", Master Thesis, The Pennsylvania State University, 2004.
40. D.F. Gill, D.L. Aumiller, D. P. Griesheimer, "Monte Carlo and Thermal-Hydraulic Coupling Via PVMEXEC," Proceedings of PHYSOR 2014, Kyoto, Japan, (2014).